

X4855934

REPORT NO. IAEA-R-2721-F

TITLE

Measurements and calculations of neutron spectra
and neutron dose distribution in human phantoms

FINAL REPORT FOR THE PERIOD

1980-11-15 - 1984-07-31

AUTHOR(S)

J. Pálfalvi

INSTITUTE

Central Research Institute for Physics
Hungarian Academy of Sciences
Budapest
Hungary

INTERNATIONAL ATOMIC ENERGY AGENCY

DATE November 1984

CERTIFIED BY:

J. M. L. L. L.

Final report
IAEA Research Contract No. 2721/R1/R2/RB

Title of Project

Measurements and Calculations of Neutron Spectra
and Neutron Dose Distribution in Human Phantoms

Health Physics Department
Central Research Institute for Physics
P.O.Box 49, Budapest 114,
H-1525, Hungary

Chief Scientific Investigator
J. Pálfalvi

Time period
15th Nov. 1980 - 31st July 1984

1. DESCRIPTION OF RESEARCH CARRIED OUT

1.1. Introduction

The measurement and calculation of the radiation field around and in a phantom, with regard to the neutron component and the contaminating gamma radiation, are essential for radiation protection and radiotherapy purposes.

To elaborate a reliable system for assessment of the necessary dosimetric quantities when evaluating a real case of a radiation accident or planning an irradiation for therapy one needs to consider the following developments:

- i/ simple detector system, sensitive mainly to neutrons with known gamma sensitivity;
- ii/ simple detector system, sensitive mainly to gammas with known neutron sensitivity;
- iii/ automatized detector measuring facilities;
- iv/ computerized evaluating system.

The developing work includes the calibrational procedures of the detectors and interlaboratory or international intercomparisons as well. The results obtained must be compared to those published by other institutions and a data bank - a compendium in other word - should be produced from them.

1.2. Detector development

1.2.1. Neutron detection

Two systems had to be developed, one for mapping the dose distribution inside an adequately chosen, human like phantom, the other for use as a personal dosimeter.

A solid state nuclear track detector system was chosen for measuring the neutron flux density inside the phantom. The system contains recoil track detectors and track detectors with internal and external (n, α) radiators. The main advantage of these detectors is the small volume, the insensitivity to gamma radiation and the low effective atomic number thereby avoiding any disturbing effect on the radiation field to be measured.

The requirements for the personal dosimeter were: to be useful for both the accident and working level dosimetry purposes, to be capable for obtaining a rough neutron spectrum from the detectors' reading, to measure the gamma dose as well. During the development work three versions were introduced and tested in several ways. They participated on three international intercomparisons. The final version is discussed in the attached report about the 5th International NAD Intercomparison cosponsored by the IAEA.

More detailed descriptions of detectors developed are in the progress report No.4 and in publications listed:

- i/ work done and published before this research contract: Publications 1-5.
- ii/ work done and published under this contract: Publications 6-10. (Sent the Agency when issued.) In Hungarian as an Institute Report: Publications 11-13. (Enclosed.)

1.2.2. Gamma detection

Most of the neutron sources emit also gamma radiation and there are neutron interreaction with detector

materials and with the tissue itself which produce gamma rays - therefore it is required to measure them, as well. For this purpose thermoluminescent (TL) materials were used. However, many of them are more or less sensitive also to neutrons. We investigated the neutron sensitivity of several TL materials under this contract and published the results in Publ. 14 (sent the Agency when issued) and in Hungarian in Publs. 15-17. (Enclosed.)

1.3. Detector measuring facilities

The construction of a semi-automatic track detector reader was performed before the research contract. It is described in Publ. 3.

To evaluate the TL detectors a portable TL reader was developed before the contract and improved during this contract. It is detailed in Publ. 18. Using the money supplied by the Agency during the first contract year also our Harshaw made TL reader was improved.

1.4. Calculational background

The External Dosimetry Group of the Health Physics Dept. developed computer programs for neutron shielding and spectrum calculations under a previous Research contract with the Agency. We adapted a neutron spectrum unfolding program, as well, to evaluate measurements. These works were published by the Agency in the Technical Reports Series No. 180.

However, these codes were not adequate for the spectrum calculations inside a phantom or to evaluate track detector measurements. They had to be and were

improved. (See also progress reports 1, 2 and 4.)

Some details about this work done under this contract were published in Publs. 19-20.

As the result of our developing work a computer program system was constructed which can be seen in Fig. 1. In Fig. 1. there is a reference to a "compendium" (Publ. 21) which contains detector responses and flux-to-dose conversion factors, among many other data. A large part of the quantities were obtained also under this contract.

1.5. Denth dose experiments

For the experiments a chest phantom was made of 5 mm thick lucite and filled with distilled water. The minor and major axes were 21.5 and 29 cm, respectively, and the height was 60 cm. Detectors were placed at different sites in the phantom. However, during a given run only two or three dosimeters were used to avoid the influence of one dosimeters on the other. For the irradiations neutron sources listed below were used.

Light water moderated critical assembly (ZR-6)
at CRIP,

Light water moderated teaching reactor (BME) at
Technical Univ. of Budapest,

Heavy water moderated critical assembly (RB) at
Vinca, Yugoslavia,

Bare ^{252}Cf source at NBS, Washington D.C., USA,

Heavy moderated ^{252}Cf source at NBS,

Radioactive neutron sources (Pu-Be, Ra-Be) at CRIP,

14 MeV neutrons from (d,T) reaction at Nuclear
Research Institute, Debrecen, Hungary,

3.2 MeV neutrons from (d,d) reaction at
The Univ. of Dresden, GDR,
6 MeV neutrons from (d,Be) reaction (Cyclotron
U-120) at Nuclear Research Institute,
Rosendorf, GDR.

In many cases the irradiations were repeated until sufficient reliable data were obtained.

The detector evaluations were performed in the laboratory of our group at CRIP.

All the experiments planned have been carried out.

1.6. Depth dose calculations

The modified version of the O5R5S program is capable to handle sources emitting neutrons in broad parallel beam or from a point source located at any distance (SSD) from the phantom surface and with or without collimator.

In the practice the irradiation geometry may be different from the theoretically possible versions therefore it is important to study the dose distribution dependence on the irradiation circumstances. This has been done for all those experiments listed in 1.5 and for many other cases. The results are tabulated.

1.7 Neutron spectrum calculations

The code O5R5S is useful for calculating also neutron spectrum inside and on the front and rear surfaces of the phantom.

The latter spectra are essential to calculate the albedo response of dosimeters worn on the body. Such spectra were calculated for monoenergetic neutrons in the energy range of 10 keV to 14 MeV for board parallel beam and for a point source with SSD of 50 cm without collimator. These spectra were already incorporated in an Agency publication (Publ. 21)

The spectra inside the phantom are important in order to calculate the mean quality factor from place to place and to calculate the isodose curves or the radiation burden of the body-organs in terms of dose equivalent. From these spectra one can calculate also the dose equivalent index (the quantity suggested by the ICRU for characterizing the radiation field in the place of the phantom).

2. RESULTS OBTAINED

The calculations and measurements resulted in many depth dose distributions, averaged detector responses and spectra and several per cents have been published only in Rubls. 19-22 (sent the Agency when issued) and in Hungarian in Rubls. 23-25 (enclosed).

The results are being prepared for publication by the Agency in the form of a Technical Document with the following list of contents.

Contents of the Technical Document entitled:
"Neutron Depth Dose Data for Health Physics Purposes".

1. Quantities and Units

- 1.1 Kerma (Fluence-to-tissue kerma conversion factors for a small volume material in free space, dosimeter reading-to-tissue kerma conversion factors for a given depth in a phantom);
- 1.2 Absorbed dose (ratio between absorbed dose and kerma);
- 1.3 Dose Equivalent (ratio between dose equivalent and kerma);
- 1.4 Dose Equivalent Index (for the ICRU spherical phantom, for an elliptical cylinder).
- 1.5 Dose from the $H(n, \gamma)D$ reaction inside the phantom
2. Dependence of dose distributions on the relative geometry of the neutron source and of the phantom (broad parallel beam, point source, collimated beams, isotropic distribution, etc.), (theory and results of Monte Carlo calculations for monoenergetic neutrons), (tables and illustrative plots);
3. Dependence of dose distributions on the shape, dimensions and material of the phantom (theory and comparative results of Monte Carlo calculations for monoenergetic neutrons), (mainly plots);
4. Neutron spectra inside and on the front and rear surfaces of the phantom.
5. Description of existing neutron sources (source geometry, beam diameter etc.) considered to be important for health physics purposes (radioactive sources: Pu-Be, Ra-Be, Am-Be etc; ^{252}Cf sources: bare and moderated; neutron generators: D-D, D-T, D-Be, etc.)
6. Comparative study on dose distributions in different phantoms for the above mentioned neutron sources (calculated and measured), (Results to be presented in plots).
7. Detector reading-to-dose equivalent index conversion factors for several commonly used detectors (TL, SSNTD).
8. Neutron dose measuring techniques inside phantoms (TL and SSNTD, fission chamber, semiconductors etc.)
9. Monte Carlo codes used for the calculations (short description of codes).
10. List of relevant literature
11. List of references
12. Index

3. CONCLUSION DRAWN

During the calculations and experimental work /which lasted for 4 years and the results have been partly published / the main directions of the investigations were as follows:

- Comparison of the direct dose distribution calculations with the experimentally obtained results in order to verify the mathematical model. There is generally good agreement /within the experimental errors/ in those cases when the real irradiation geometry could have been taken into account by the model /Figs. 2, 4, 5/. In those cases when the measures of the source and of the phantom were comparable and the SSD was short the deviation was significant near the front surface /Figs. 3, 6/.
- Dependence on SSD which clearly can be seen in the cases of the uncollimated point sources; for short SSDs the kerma inside the phantom decreases much more rapidly than for the longer ones /Figs. 5, 8/.
- How the dose build up and attenuation are effected by the fraction of fast neutrons to the intermediate and thermal ones in the spectrum /Figs. 7, 8/.
- How strong is the dependence of the dose distribution on the neutron spectrum. For the uncollided ^{235}U and ^{252}Cf fission spectra a slight difference was found by calculations but practically no differences can be seen between the different $\alpha\text{-Be}$ sources; the measurements cannot distinguish these source spectra from each other at all /Figs. 2, 5/. The use of quite different absorbers to the same source, however, can result in significant effects /Fig. 9/.
- Reproducibility of experiments; it was found that even using the standardized evaluation procedure /see Fig. 1/ the new result can be out of the experimental error limits. The main reasons are the uncertainty in positioning the detectors inside the phantom and the different scattering effects from the structural elements in the experimental hall /Figs. 4, 6/.
- It was the purpose to find quantities characteristic from dosimetrical point of view. Such a quantity might be the depth of the half value of the kerma inside the phantom. How this quantity varies against the variation of the irradiation circumstances is illustrated in Tables 1 and 2.
- Such an important information is the quality of the neutron spectrum at different depths of the phantom. It was pointed out earlier that for water moderated fission spectra no essential changes in the spectrum shape can be observed. This was found for the cases of the D_2O moderated ^{252}Cf source and the Vinča RB reactor as well. The uniformity of spectra can be characterized by the spectrum averaged flux to kerma conversion factors, it was found that for the above mentioned neutron sources this value is $2.45 \pm 0.25 \cdot 10^{-11}$ Gy $\cdot\text{cm}^2$ at any depth /Figs. 10, 11, 12/. Of course, if the SSD is small and/or the diameter of the phantom is higher than that was used by us /21.5 cm/ the shape of the spectrum and the flux-to-dose conversion factors may vary significantly even for those spectra, too, near the rear surface.
- For health physics purposes the maximum equivalent dose inside the phantom is one of the most important value. In the lack of a complicate evaluation system it can be concluded from the conversion factors. Some samples measured are shown in Table 3.

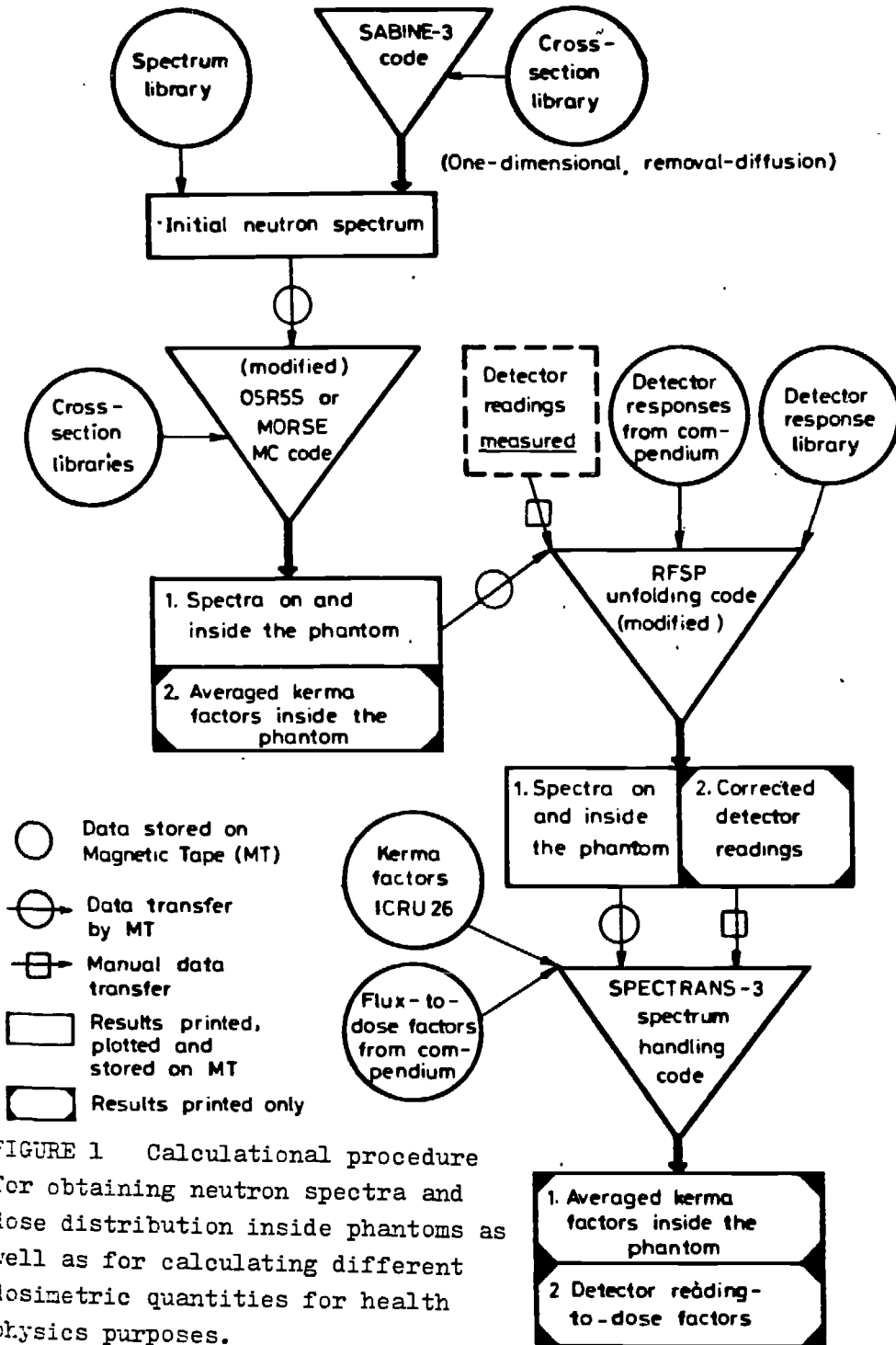


FIGURE 1 Calculational procedure for obtaining neutron spectra and dose distribution inside phantoms as well as for calculating different dosimetric quantities for health physics purposes.

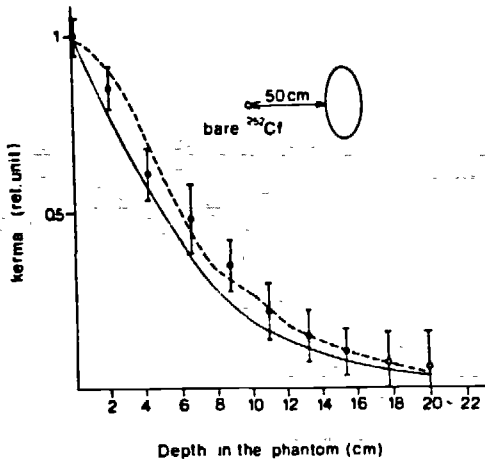


FIGURE 2 Measured /open circles/ and calculated /dashed line/ kerma distribution curves in the phantom along the minor axis when irradiated by neutrons from a bare ^{252}Cf source. The solid line was calculated for an uncollided fission spectrum.

FIGURE 3 Measured /open circles/ and calculated kerma distribution curves in the phantom along the minor axis when irradiated by neutrons from a D_2O moderated ^{252}Cf source. The dashed and solid lines were calculated for a broad parallel and an uncollimated divergent beam, resp.

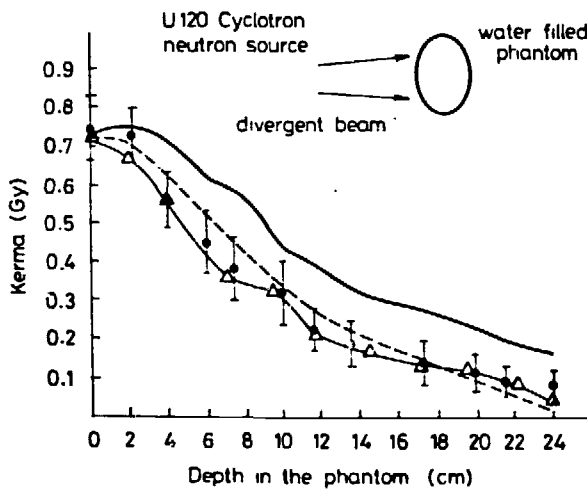
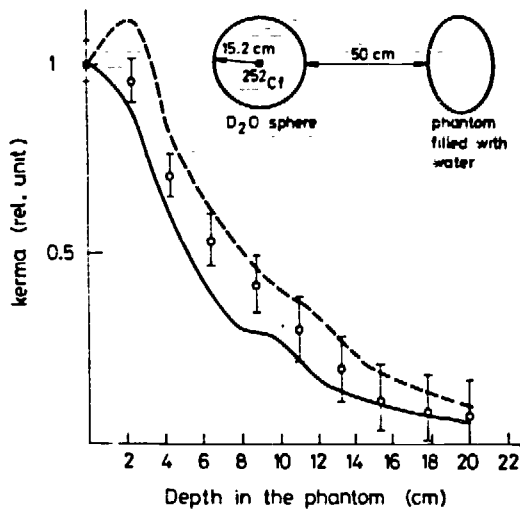


FIGURE 4 Kerma attenuation curves in the phantom along the minor axis when irradiated by neutrons with mean energy of 6 MeV produced by $/\text{D},\text{Be}/$ reaction at the Cyclotron U 120, $/Q=5000/$. The solid and dashed lines were calculated for a broad parallel and a narrow divergent beam $/\text{SSD}=100\text{ cm}, \text{FS}=15 \times 15\text{ cm}/$, resp. The solid line marked by Δ was measured by B. Dörschel, while the individual points represent the results of this work.

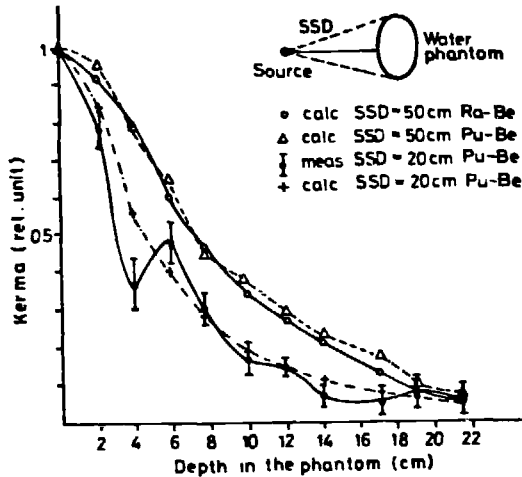


FIGURE 5 Measured /full circles/ and calculated kerma distribution curves in the phantom along the minor axis when irradiated by / α -Be/ neutron sources.

FIGURE 6 Calculated fluence to kerma conversion factors for the Vinča RB /open circles/ and Viper /full rectangle/ reactors as well as measured kerma distribution curves for the Vinča RB reactor. The phantom used was a circular cylinder with radius of 15 cm.

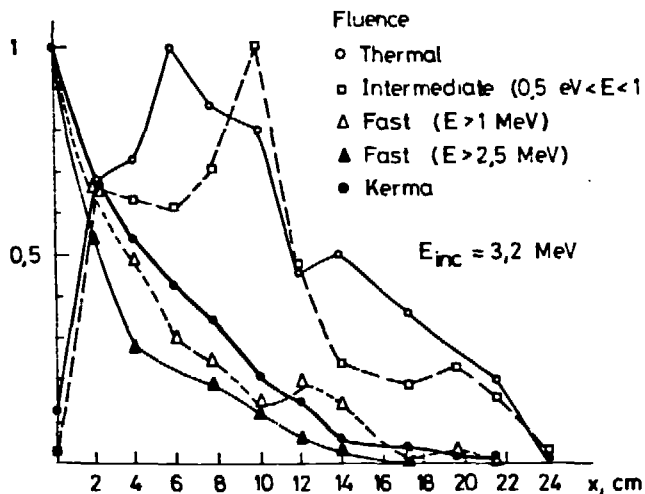
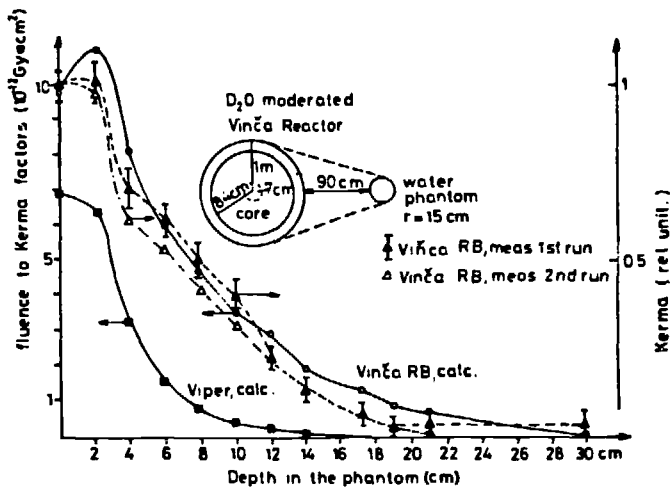


FIGURE 7 Measured kerma and flux-density distribution curves inside the phantom for neutrons with energy of 3.2 MeV originated from /D,D/ reaction /point source without collimator, SSD=10 cm/.

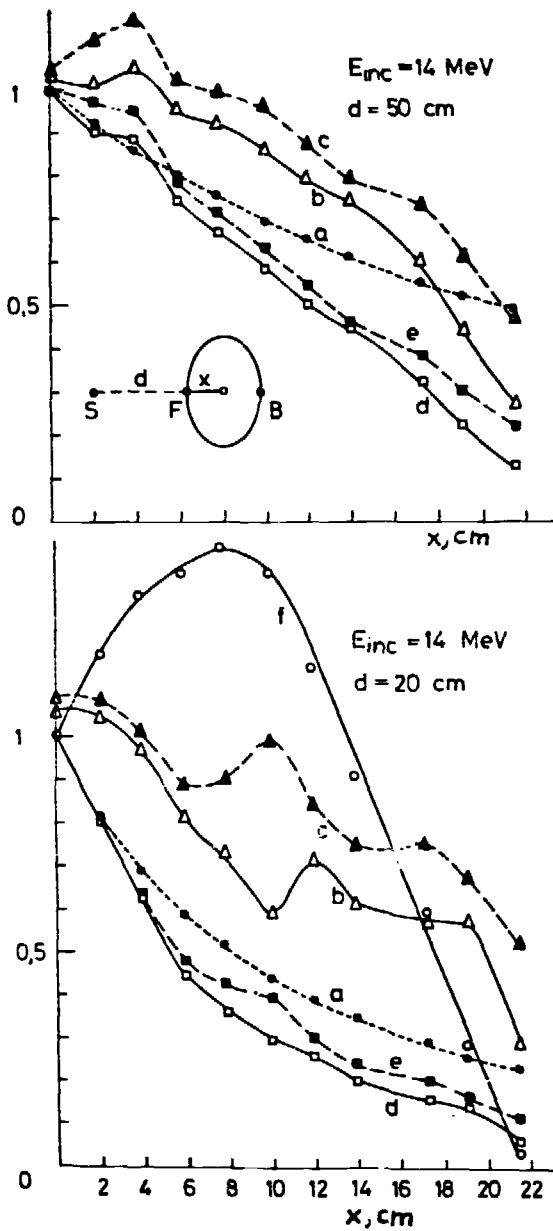


FIGURE 8 Several distribution curves obtained from the 14 MeV neutron irradiations are presented in the Fig. 8. The curve a represents the $1/(d+x)^{-2}$ function in a way that for $x=0$ its value was taken to be 1. It characterizes both the neutron fluence and tissue kerma distributions in the radiation field without the phantom. When the phantom is present the neutron scattering and other interreactions modify these distributions. The curves b and c show the relative changes to the air of the integrated fluence of neutrons with an energy threshold of 2.5 MeV and the total direct neutron tissue kerma, respectively. The values of the same quantities, but normalized to 1 at a place $x=0$, are given by the curves d and e and, in addition, the thermal neutron fluence distribution is plotted as curve f.

In both cases, the kerma has a "plato" but at different depths and there is a "build up" effect as well, which increases with increasing source distance d .

TABLE I Calculated and measured depth of the half-value of kerma relative to that given for the first volume element of the phantom on the dependence of the irradiation parameters for several calibrational and therapeutic neutron sources.

Source	C: Calc. M: Meas.	PS: point source PB: parallel beam DB: divergent beam FS: field size	Source to sur- face Distance /cm/	Depth of half- value of kerma /cm/
Fission	C	PS	50	5.2
²⁵² Cf, bare NBS, USA	C	PS	50	6
	M	-	50	6
²⁵² Cf, D ₂ O moderated NBS, USA	C	PB	-	8
	C	FS	50	5.2
	M	-	50*	7
Cyclotron	C	PB	-	13
U120, GDR /D,Be/ $\bar{E}_n = 6$ MeV	C	DB, FS=15x15 cm ²	100	9.5
	M No.1	DB, FS=12x15 cm ²	102	7
	M No.2	DB, FS=12x15 cm ²	102	8.2
14 MeV /D,T/ ATOMKI Hungary	C	PB	-	~22
	C	PS	50	13.5
	M	-	50	13
3.2 MeV /D,D/ TU Dresden GDR	M	-	20	5.6
	C	PB	-	11.5
	C	PS	50	6.5
Pu-Be or Ra-Be	M	-	10	4.5
	C	PS	50	7.2
KFKI Hungary	C	PS	20	4.6
	M	-	20	~4

* See Fig. 4

TABLE II Calculated and measured depth of the half-value of kerma relative to that given for the first volume element of the phantom for several reactor spectra.

Source	C: Calc. M: Meas.	Arrangement or absorber	Depth of half- value of kerma /cm/
LWR1	C	Detailed	10.2
KFKI, Hungary	M	in /1/	9.2 - 13 *
LWR2	C	Detailed	11.8
TU Budapest Hungary	M	in /1/	10.8
Vinca	C	See Fig. 7	7.4
RB	M No.1		8
Yugoslavia	M No.2		6.5
Viper, U.K.	C	Detailed in /5/	3
HPRR	C	bare	6.5
Cak Ridge USA	C	12 cm lucite	6.4
	C	13 cm steel	4.8
	C	20 cm concrete	6.6
	C	5 cm steel + 15 cm concrete	5.8

* measured repeatedly by different methods.

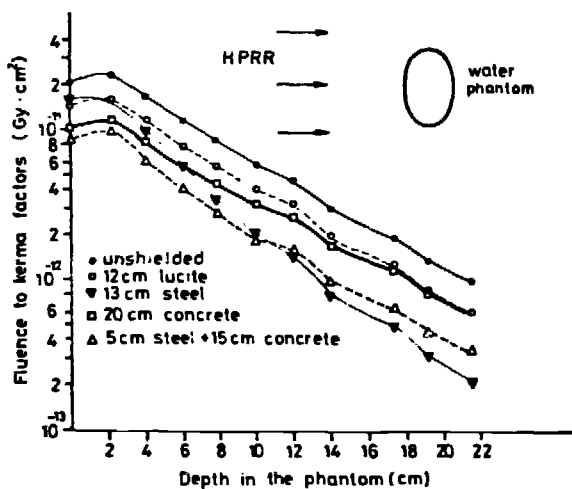
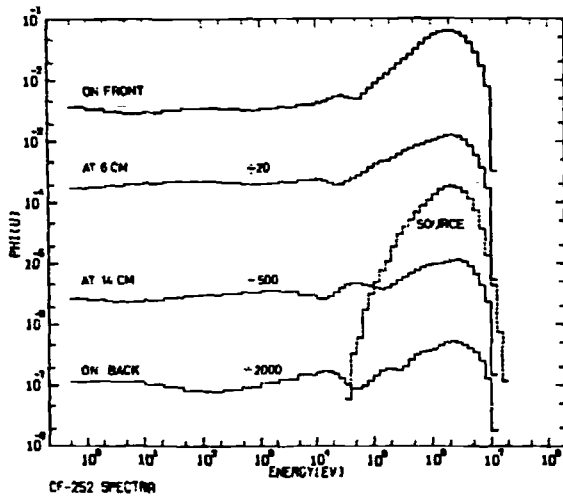


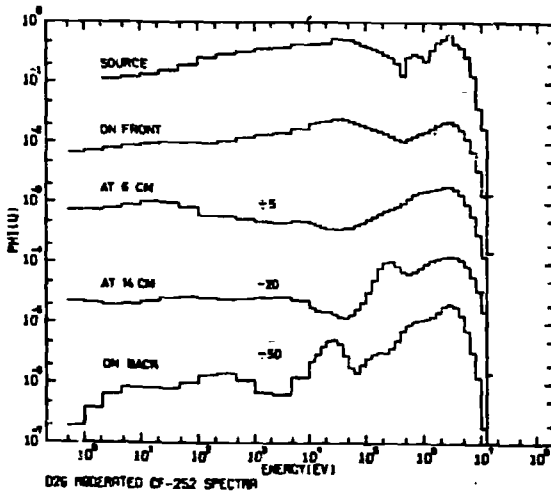
FIGURE 9
Fluence to kerma
conversion factor
attenuation curves
inside the phantom
calculated for
different HPRR
spectra.

TABLE 3 Averaged responses of several nuclear track detectors used for the experiments, expressed in terms of track density per maximum equivalent dose /cm² x Sv⁻¹/.

Source	Response /x 10 ⁶ /		
	NTA film	²³⁵ U /15%/+Lexan	CR-39 /ECE/
252-Cf bare	1.23	0.029	0.654
252-Cf, D ₂ O mod.	1.01	0.268	0.529
U-120	1.76	0.027	0.409
Pu-Be	1.65	0.016	0.476



FIGURES 10, 11
Measured neutron spectra on the front and rear surfaces and inside the phantom for various neutron sources. The plots are shifted by the factors indicated /relative to the front where $\int \phi(u) du = 1/$ in order to avoid overlapping /except the source spectra which were plotted where free room was available/.



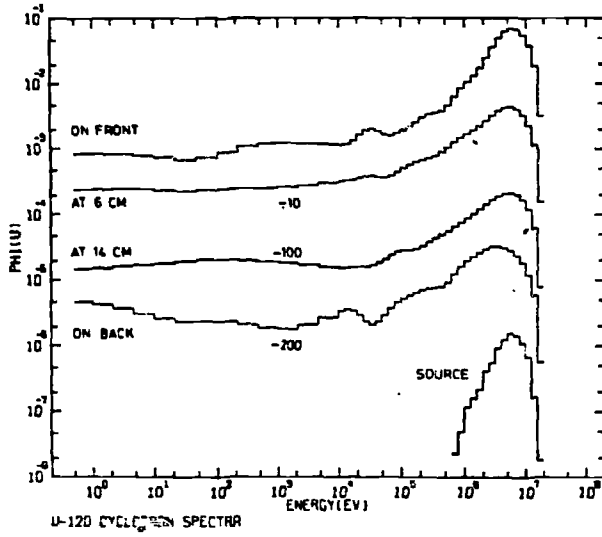


FIGURE 12
Measured neutron
spectra on and inside
the phantom for the
U 120 cyclotron.

4. LIST OF REFERENCES PUBLICATIONS

1. J. Pálfalvi, 1978, Thermal and Intermedier Neutron Flux Density Determination for Accident Dosimetry Purposes Using Thick Gold Foils, Rep. KFKI-1978-42.
2. J. Pálfalvi, 1978, Nuclear Accident Dosimetry Measurements, Czechoslovak-Hungarian Intercomparison, Budapest, Hungary, 1977, Rep. KFKI-1978-65.
3. J. Pálfalvi, I. Eördögh, B. Verő, 1980, Track Density Measurements Using a VIDIMET-II A Type Image Analyser, Nuclear Tracks Supplement No. 2, Nuclear Track Detectors ed. H. Francois et al. Pergamon Press, pp. 503-507.
4. J. Pálfalvi, 1981, On the Use of LR115 II Recoil Track Detectors for Neutron Dosimetry, Nuclear Instruments and Methods, Vol. 180, pp. 511-514.
5. J. Pálfalvi, A.M. Bhagwat, L. Medveczky, 1981, Investigations on the Neutron Sensitivity of Kodak-Pathé LR115 Recoil Track Detector, Health Physics, Vol. 41, pp. 505-512.
6. J. Pálfalvi, 1982, Neutron Sensitivity of LR115 SSNTD Using Different n, α Radiators, Nuclear Instruments and Methods, Vol. 203, pp. 451-457.
7. J. Pálfalvi, 1982, Neutron Sensitivity Calculations on Simple Albedo Track Detectors, Nuclear Tracks, Vol. 6, pp. 185-188.
8. J. Pálfalvi, 1983, Neutron Response of Several Fission Track Detectors Worn on the Body, Rep. KFKI-1983-65.

9. J. Pálfalvi, 1984, Calibration of Fission and n, α Track Detectors on Phantom, Proc. 12th Int. Conf. on SSNTDs, Acapulco, Mexico, 4-10 Sept. 1983.; Nucl. Tracks, V. 8, pp. 293-296.
10. J. Pálfalvi, 1984, Neutron Sensitivity Measurements of LR115 Track Detector with Some n, α Converters, Nucl. Tracks, V.9, pp. 47-57.
11. J. Pálfalvi, 1982, Baleseti Dozimetriai Célra Használható Radiátor Nélküli Szilárdtest-Nyomdoziméter Fejlesztés, Rep. KFKI-1982-43.
12. J. Pálfalvi, 1983, n, α Magreakción Alapuló Szilárdtest Nyomdoziméter Hatásfokának Elméleti és Kísérleti Vizsgálata, Rep. KFKI-1983-46.
13. J. Pálfalvi, 1984, n, α magreakción alapuló szilárdtest nyomdetektorokból felépített személyi albedo neutron doziméter jelzésének vizsgálata számítással, Rep. KFKI-1984-26.
14. P.P. Szabó, J. Pálfalvi, 1984, Investigation of Neutron Sensitivity of LiF and CaSO₄ Thermoluminescent Detectors, Nucl. Tracks, V.9, pp. 59-67.
15. P.P. Szabó, J. Pálfalvi, 1982, Rutin személyi dozimetriában használt LiF TL detektorok termikus neutronérzékenységének vizsgálata a ZR-4-es reaktor termikus oszlopában, Rep. KFKI-1982-41.
16. P.P. Szabó, J. Pálfalvi, 1983, A LiF és a CaSO₄ termolumineszcens detektorok neutronérzékenységének vizsgálata, Rep. KFKI-1983-45.

17. P.P. Szabó, J. Pálfalvi, 1984, Termolumineszcens detektorok gyorsneutron érzékenységének vizsgálata, Rep. KFKI-1984-36.
18. B. Szabó et al., 1982, The TLD-04B-TC Thermoluminescent Reader for Research and Routine Dosimetry Applications, Isotopenpraxis V. 18, pp. 98-102.
19. J. Pálfalvi, L. Koblinger, P.P. Szabó, 1983, Depth-Dose Distribution Measurements and Calculations in an Elliptical Phantom, Health Physics, Vol. 44, pp. 35-44.
20. J. Pálfalvi, 1984, Neutron Depth Dose Calculations and Measurements in an Elliptical Phantom for Radiation Protection Purposes, 5th Symp. on Neutron Dosimetry, Neuherberg, FRG, Sept. 17-21, 1984.
21. R.V. Griffith, J. Pálfalvi, U. Madhvanath, 1983, Compendium of Neutron Spectra and Detector Responses for Radiation Protection Purposes, IAEA Technical Reports Series, in press.
22. J. Pálfalvi, 1982, Neutron Dose Distribution Measurements in a Water Filled Phantom by SSNTDs, Nuclear Tracks Supplement No. 3, Nuclear Track Detectors ed. P.H. Fowler et al. Pergamon Press, pp. 481-485.
23. J. Pálfalvi, L. Koblinger, 1982, Neutronspektrum és dóziseloszlás vizsgálatok - számítással és méréssel - elliptikus fantomban, könnyűvízzel moderált reaktor spektrumban, Rep. KFKI-1982-42.

24. J. Pálfalvi, 1983, Neutronspektrum és dóziseloszlás vizsgálatok számítással és méréssel elliptikus fantomban ^{252}Cf és nehézvízzel moderált ^{252}Cf neutron forrásokra, Rep. KFKI-1983-47.
25. J. Pálfalvi, 1984, Neutron spektrum és dóziseloszlás vizsgálatok számítással és méréssel elliptikus fantomban ciklotron, 3,2 MeV és 14 MeV energiájú neutronokra, Rep. KFKI-1984-27.

20th Nuclear Accident Dosimetry
Intercomparison^{**}

Oak Ridge National Laboratory
September, 1983

J. Pálfalvi

Central Research Institute for Physics
Health Physics Department^{***}
P.O.Box 49, Budapest 114, 1525
Hungary

^x Sponsored by the IAEA as the 5th Int. NAD Intercomparison

^{xx} The work was partly supported by the IAEA Research
Contract No. 2721/R2/RB/

I. Description of the accident dosimeter used in the CRIP

The detectors of the dosimeter are located in a thin and flat box made of polypropilene as shown in Figs. 1 and 2.

The relatively thick gold foil (200 mg/cm^2) is to be used for a first and quick monitoring of persons in a case of an accident, while the gold-cadmium-gold sandwich is for the thermal and intermediate neutron fluence determination. The use of this system is suitable not only for measuring neutrons entering the body but also enables us to estimate the neutron fluence emerging from the body and in this way it indicates the fast neutron component, as well. The technique is based on the observation that the beta activity distributions induced by both incident and reflected thermal and intermediate neutrons are different for the two gold foils as illustrated in Fig.3. By measuring the beta radiation from both sides of each gold foil and using appropriate conversion factors the fluences required can be obtained. More detailed informations and conversion factors are available from /1/.

The sulphur pellet and the ^{232}Th -Makrofol E (or Lexan) fission track detector are used for the fast neutron fluence determination with thresholds of about 2.5 and 1.5 MeV, respectively. The ^{132}Th converter was manufactured of ThO_2 with an effective thickness of 9 mg/cm^2 painted on a thin Al holder.

LiF powder (Harshaw TLD-700) is used for gamma dose measurements.

In addition, three different solid state track detectors were placed in the same box as follows:

- LR115 II type cellulose nitrate (Kodak-Pathé) track detector which utilizes the direct neutron interactions with the detector material (mainly neutron-alpha reactions and recoil C,O and N ions). This is considered as a fast neutron detector with a practical threshold of about 0.8 MeV /2,3/;

- depleted uranium foil (with 380 ppm ^{235}U content) as a converter and Lexan polycarbonate for the induced fission fragments detection. This is also a fast neutron detector with a threshold of 1 MeV /4/.

- a Cd covered (neutron-alpha) track detector which contains a LiF converter and a LR115 II type plastic foil for registering the neutron induced alpha particles. This is considered to be an $1/v$ detector with a cadmium cut off of 0.5 eV /5,6/.

The detailed measuring techniques of these detectors are given in the publications presented above.

In general, the neutron dose determination can be done in three different ways:

- From the measured beta activity of gold and sulphur detectors assuming an $1/E$ and a Maxwellian spectrum for the intermediate and fast neutrons, respectively one can obtain fluence values and using averaged fluence-to-dose conversion factors;
- from known irradiation circumstances one can assume a more reliable neutron spectrum and following the previous method;
- measuring the reading of all the detectors located in the dosimeter and assuming a neutron spectrum as a first approximation one can use an unfolding computer program for obtaining the most real neutron spectrum and fluence-to-dose conversion factors averaged over that spectrum.

In the case of this accident dosimetry intercomparison study the 2nd version was used for the immediate dose assessment in the DOSAR Laboratory and the 3rd method was applied for the final dose determination and performed in the CRIP in Hungary.

II. Dose determination using Au and S detectors

The beta activity of detectors were measured first in the DOSAR Laboratory using an end-window GM counter. However, the counting geometry and the GM tube were different from ours, therefore the facility had to be calibrated for our evaluation system given in /1/. For this we used gold foils and sulphur pellets irradiated and their activities measured by our calibrated systems in Hungary.

A correction had to be made owing to the differences in the distances between the GM tube's end-window and the detector surface to be measured. In Hungary these distances were of 6.5 and 10.8 mm

for gold and sulphur, respectively; at the DOSAR's counter 4, 20.5 and 37 and 53.5 mm distances were available.

As a first step we established that the counting rate varied exponentially with the distance (x) in the form $a \cdot \exp(mx)$. For m (the slope of the function in a lin-log representation) the value of -0.0469 ± 0.0003 was found by exponential regression, which was slightly different from that used at home (-0.0448) showing a negligible differences between the two GM tube arrangements.

The detectors with known beta activity were measured again either in a 4 or in a 20.5 mm distances (x) according to their counting rate to avoid both the low and high values which might result in a poor statistics or a need for dead time correction. Then, the measured values (c) were transformed to 6.5 or 10.8 mm distances by the formula;

$$C'_{g \text{ or } s} = C \cdot \exp(m(x'-x)), \quad /1/$$

where $x'=6.5$ or 10.8 for gold and sulphure, respectively.

Considering our device, this counting rate for gold should have been C'_g (taking into account the desintegration too) and thus a $k'_g = C'_g / C'_g$ correction factor was obtained. Following this, both sides of gold foils were measured, the counting rates were transformed by the formula /1/, corrected for the desintegration and substituted into the equations;

$$\phi_I = (277C'_3 - 282C'_2 - 31.6C'_c + 31C'_d) k'_g l, \quad /2/$$

$$\phi_{th} = (-780C'_3 + 1360C'_2 + 581C'_c - 558C'_d) k'_g l,$$

where ϕ_{th} is the thermal neutron fluence in cm^{-2} ,

ϕ_I is the intermediate fluence per unit lethargy in cm^{-2} ,

C'_3 , C'_2 , C'_c and C'_d are the final counting rates corresponding to the gold foil faces taken consecutively from the top of the detector,

$l = 1/F\lambda$, when F is the area of the foil in cm^2 and λ is the desintegration constant in s^{-1} .

The numerical values in the equations refer to the foil thickness of 100 mg/cm^2 (and can be different for other foil thicknesses as can be seen in /1/).

To obtain the neutron dose in the energy range of 0.5 eV - 1 MeV (D_I) the following method was used:

1. The neutron spectra were considered to be known and were taken from the literature /7/;
2. The $r = \phi'_r / \phi'_{tot}$ fluence ratios were calculated from the spectra;
 ϕ'_r : the fluence in the 0.5 eV - 10 eV energy interval and
 ϕ'_{tot} : the fluence in the 0.5 eV - 1 MeV interval, both taken from the spectrum;
3. ϕ_{tot}^I , the real fluence in the 0.5 eV - 1 MeV interval, was obtained by $\phi_{tot}^I = 3 \cdot \phi'_r / r$, here 3 is the lethargy length of the 0.5 eV - 10 eV interval;
4. and finally the dose came from the expression:

$$D_I = (k_n + k_\gamma) \phi_{tot}^I, \text{ where } k_n \text{ and } k_\gamma \text{ are the neutron absorbed dose and the neutron induced gamma dose conversion factors for the 57th volume element of the Snyder phantom and both averaged over the spectra in the energy range from 0.5 eV to 1 MeV. The conversion factors were taken from the IAEA Technical Report No. 180 /3/.$$

In the case of sulphur the same method was followed as for the gold to obtain, at first, the corrected counting rates (C'_a) and using the $k_s = C_s / C'_s$ correction factor the fast neutron fluences (above the 2.5 MeV threshold) were calculated by the expression:

$$\phi'_F = k_s \frac{C'_a \cdot S}{\bar{\sigma} \cdot m_s}, \quad /3/$$

where $S = 2.3 \cdot 10^9$ (calibration constant), m_s is the mass of the pellet in g, and $\bar{\sigma}$ is the averaged $^{32}\text{S}(n,p)^{32}\text{P}$ reaction cross-section in barn. Calculating the fluence ratio from the spectrum $r = \phi'_r / \phi'_{tot}$, where ϕ'_r : the fluence of neutrons above 2.5 MeV and

ϕ'_{tot} : the fluence of neutrons above 1 MeV, the real fluence above 1 MeV neutron energy can be deduced by the expression:

$$\phi_{tot}^F = \phi'_F / r \quad \text{and the dose } D_F = (k'_n + k'_\gamma) \phi_{tot}^F, \text{ where}$$

k'_n and k' are similar quantities to those used earlier but averaged above 1 MeV neutron energy.

The total neutron dose is the sum of D_I , D_F and of $(k'_n + k')\phi_{th}$, where the latter term means the thermal neutron dose.

During each irradiation 2 dosimeters were mounted on each phantom and in free air position too. The dose values for the three irradiations are summarized in Table 1 together with the reference dose values supplied by the staff of the DOSAR Laboratory after the evaluation. Our values are the averages of those obtained from the evaluation of 4 and 2 dosimeters for phantoms and free air, respectively. Errors were not estimated because these dose data were considered to be preliminary ones.

		PULSE		
		No. 1 bare	No. 2 13 cm iron	No. 3 20 cm concrete
Free air	Ref.	375	103	51
	CRIP	366	146	50
Phantom	Ref.	430	141	59
	CRIP	453	177	69

Table 1

The dose values are given in rads.

In the case of phantoms the absorbed doses are presented for the 57th element of the Snyder phantom, including the dose from the neutron induced gamma rays. For the free air irradiations the tissue kerma are given. However, in all cases the "reference values" does not contain the neutron induced gamma doses.

III. Final dose determination

3.1 Neutron dose

The activity of the activation detectors was high enough to enable us for measuring it by our standardized devices in the CRIP

several days later. From these measurements we recalculated the thermal neutron fluences and doses by the same method described in the previous section. The beta counting rates from both the gold foils and sulphur pellets were used as one part of the input data to the neutron spectrum unfolding code RFSP-Jul as well.

As next step, all the track detectors were evaluated following the methods given in the publications listed in the first section /2,3,4,5,6/. The measured track densities formed the second part of the input data to the code RFSP-Jul. The response functions -given also in the listed papers- had been incorporated in the code as an additional subroutine to improve the code to handle not only activation detectors. As input spectra those used for the first dose estimation were used. The output of the code gives the unfolded neutron spectra, the averaged fluence-to-dose conversion factors and the actual dose values, i.e. tissue kerma; absorbed dose (D_n), H(n,gamma)D dose (D_y) and dose equivalent (H) for the 57th volume element of the Snyder phantom as well as the dose equivalent index (H_T) for the ICRU spherical phantom. In addition, the total neutron fluences above the cadmium cut off (0.5 eV) and the fluences in several predetermined energy ranges can be obtained by the code.

The fluence and dose values obtained are presented in Table 2. The errors given are the estimated statistical errors evaluated from the detector measurements (including the calibration uncertainties of the facilities).

There are several comments to the Table 2 as:

- The incident thermal fluences include the scattered neutrons from the half space in front of the detectors.
- The scattered thermal neutrons come from the half space behind the detector when irradiated in "free air".
- The reflected thermal fluences mean the fluences of neutrons slowed down by and reflected from the phantom.
- The intermediste fluences include the incident and reflected fluences too and therefore these values are higher for phantom irradiations than for free air cases. However, this effect is significant only in the 0.5 eV - 2 keV energy range.
- Where errors are not given the values were calculated from the unfolded neutron spectra.

		Neutron Fluences in 10^{10} n/cm ²			
		run No.1 bare	run No.2 13 cm iron	run No.3 20 cm concrete	
FREE AIR	Thermal Incident [ⓐ]	0.253	0.115	0.529	Errors 4 - 13 %
	Scattered	0.240	0.098	0.293	
	Total	T: 0.493	T: 0.213	T: 0.823	
	Intermediate 0.5eV-2keV	0.910	0.536	1.07	
	2keV-150keV [ⓐ]	1.59	1.34	1.49	
	150keV-1MeV [ⓐ]	6.73	6.74	0.84	
	Fast 1MeV-2.5MeV [ⓐ]	4.58	1.56	0.505	
	> 2.5MeV [ⓐ]	2.22	0.318	0.295	
	Total > 0.5eV kerma (Gy)	T: 16.03 ± 1.25 3.43	T: 10.50 ± 1.27 1.69	T: 4.20 ± 0.70 0.462	
	PHANTOM	Thermal Reflected	2.29	1.20	
Total		T: 2.54	T: 1.32	T: 1.60	
Intermediate 0.5eV-2keV		4.04	1.92	1.85	
Total > 0.5eV		T: 19.16 ± 1.60	T: 11.88 ± 1.40	T: 4.98 ± 0.91	
D _n (Gy)		3.83	1.75	0.508	
D _T (Gy)		0.41	0.30	0.139	
H (Sv)		40.4	19.8	5.38	
H _T (Sv)		41.2	21.3	5.46	

[ⓐ]The same values for the phantom, too

Table 2

3.2 Gamma dose

For the gamma dose measurements we used only ^7LiF powder (TLD-700, Harshaw). The TL-detectors were evaluated by a reader type TLD-04B-TC (/9/, made in Hungary). For calibration a secondary standard ^{60}Co gamma source was used.

The composition of the powder was investigated by mass spectrometry method and a 450 ppm ^6Li contamination was found. The neutron response, $R(E)$, of this material was determined by experiments using monoenergetic neutron sources (from thermal up to 14 MeV) /10,11,12/ and the following analytical expressions were established:

$$\text{for thermal} : R(E) = 2.25 \cdot 10^{-9} \text{ mGy} \cdot \text{cm}^2,$$

$$\text{from thermal up to 2keV} : R(E) = 1.5 \cdot 10^{-11} \cdot E^{-0.285} \text{ mGy} \cdot \text{cm}^2,$$

$$\text{from 2keV up to 150keV} : R(E) = 1.10 \cdot 10^{-10} \text{ mGy} \cdot \text{cm}^2,$$

$$\text{from 150keV up to 20MeV} : R(E) = 1.1 \cdot 10^{-9} \cdot E^{1.24} \text{ mGy} \cdot \text{cm}^2,$$

where E is the neutron energy in MeV.

In mixed neutron-gamma field these functions can be used for correcting the TL reading for neutrons. After measuring the neutron spectra, $\phi(E)$, and fluences (ϕ_j) the averaged TL responses (\bar{R}_j) for each energy interval (E_i, E_k) can be calculated by the formula:

$$\bar{R}_j = \frac{\int_{E_i}^{E_k} R(E) \phi(E) dE}{\int_{E_i}^{E_k} \phi(E) dE}$$

and the TL reading induced by neutrons can be obtained:

$$R = \sum_j \phi_j \bar{R}_j$$

This value should be subtracted from the total TL reading (or apparent gamma dose, in other words) to obtain the real gamma dose.

In Table 3, we summarize the TL measurements.

The statistical errors of the TL measurements were less than 10 % (including the calibration error of the ^{60}Co equipment).

		Corrections for neutrons (mGy _{air})						
Apparent † dose mGy _{air}		Thermal	0.5eV- 2keV	2keV- 150keV	150keV	Total	Final † dose mGy _{air}	
Run No.1								
Phantom	1072	57	21	1.6	265	344	728	
free air	551	11	4.7	1.6	265	282	269	
Run No.2								
Phantom	339	30	8.7	1.3	76	116	224	
free air	122	4.8	2.4	1.3	76	84	38	
Run No.3								
Phantom	344	36	12	1.5	36	86	258	
free air	179	19	7.0	1.5	36	63	116	

Table 3

IV. Acknowledgements

Thanks are due to the IAEA for organizing this International Intercomparison and for the financial support in the participation and to the staff of the DOSAR Laboratory (ORNL), in particular the author is very grateful to Drs C.S. Sims, R.Swaja and G.R. Patterson for their direct help during the irradiations and evaluations.

V. References

- /1/ J.Palfalvi,1978, Thermal and Intermediate Neutron Flux Density Determination for Accident Dosimetry Purposes Using Thick Gold Foils, Rept. CRIP No. KFKI-1978-42.
- /2/ J.Palfalvi,1981, On the Use of LR115 II Recoil Track Detectors for Neutron Dosimetry, Nucl.Instr. V.180,pp.511-514.

- /3/ J.Palfalvi, A.M. Bhagwat, L. Medveczky, 1981, Investigations on the Neutron Sensitivity of Kodak-Pathé LR115 Recoil Track Detector, Health Physics V.41, pp.505-513.
- /4/ J.Palfalvi, 1983, Neutron Response of Several Fission Track Detectors Worn on the Body, Rept. CRIP No. KFKI-1983-65.
- /5/ J.Palfalvi, 1982, Neutron Sensitivity of LR115 SSNTD Using Different (n, alpha) Radiators, Nucl. Instr. V.203, pp.451-457.
- /6/ J.Palfalvi, 1982, Neutron Sensitivity Calculations on Simple Albedo Track Detectors, Nuclear Tracks V.6, pp.185-188.
- /7/ C.S. Sims, G.G. Killough, 1981, Reference Dosimetry for Various Health Physics Research Reactor Spectra, Rept. ORNL No. ORNL/TM-7748.
- /8/ R.V. Griffith, J.Palfalvi, U. Madhvanath, 1983, Compendium of Neutron Spectra and Detector Responses for Radiation Protection Purposes, IAEA Technical Reports Series, in press.
- /9/ B. Szabo et al, 1982, The TLD-04B-TC Thermoluminescent Reader for Research and Routine Dosimetry Applications, Isotopenpraxis V.18, pp.98-102.
- /10/ P.P. Szabo, J.Palfalvi, 1982, Neutron Response of LiF TL Detector, Rept. CRIP No. KFKI-1982-41.
- /11/ P.P. Szabo, J.Palfalvi, 1984, Investigations on Neutron Sensitivity of LiF and CaSO₄ Thermoluminescent Detectors, Nuclear Tracks, V.9, pp. 59-67.
- /12/ P.P. Szabo, J.Palfalvi, 1983, Fast Neutron Sensitivity of Several TL Materials, Rept. CRIP, No. KFKI-1983-45.

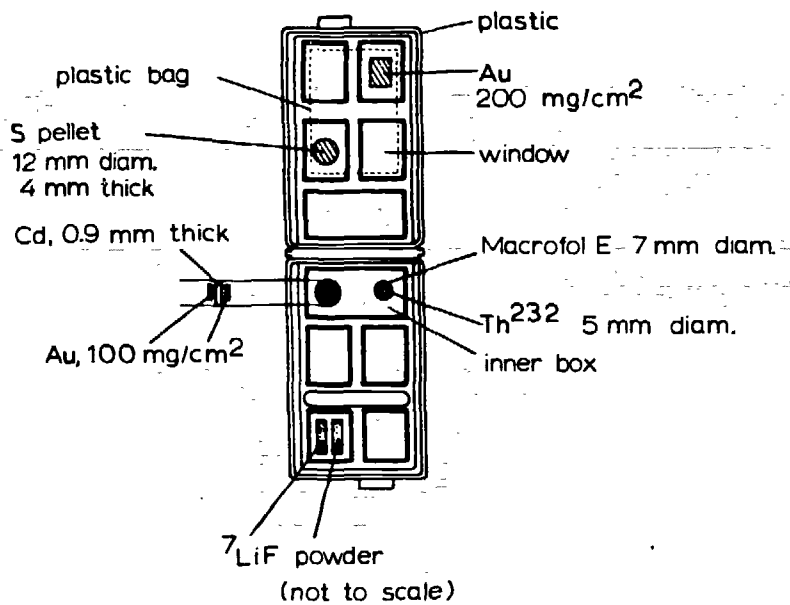


fig. 1

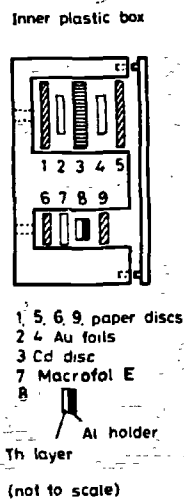


fig. 2

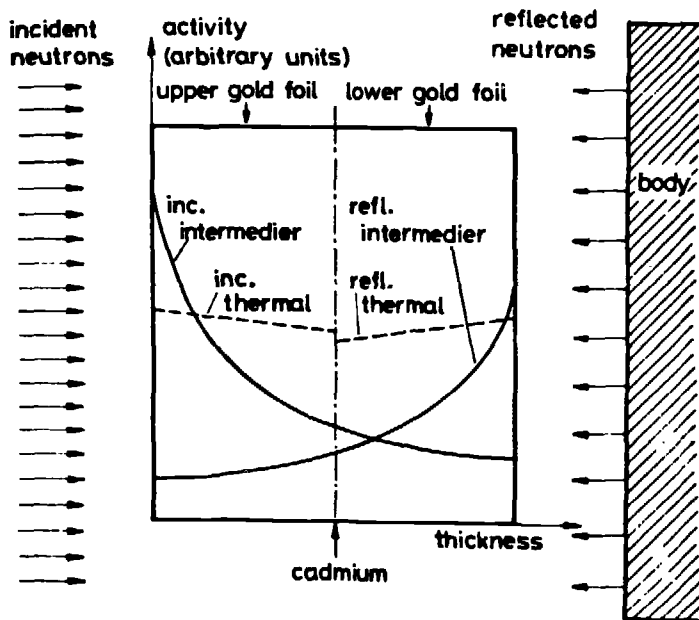


fig. 3